Van der Waals interaction and spontaneous decay of an excited atom in a superlens-type geometry

Agnes Sambale and Dirk–Gunnar Welsch
Theoretisch–Physikalisches Institut, Friedrich–Schiller–Universität Jena, Max–Wien-Platz 1, D-07743 Jena, Germany

Ho Trung Dung
Institute of Physics, Academy of Sciences and Technology,
1 Mac Dinh Chi Street, District 1, Ho Chi Minh city, Vietnam

Stefan Yoshi Buhmann
Quantum Optics and Laser Science, Blackett Laboratory, Imperial College London,
Prince Consort Road, London SW7 2BW, United Kingdom
(Dated: November 28, 2008)

Within the framework of macroscopic quantum electrodynamics, the resonant van der Waals potential experienced by an excited two-level atom near a planar magneto-electric two-layer system consisting of a slab of left-handed material and a perfect mirror is studied. It is shown that disregarding of material absorption leads to unphysical results, with divergent values for the potential away from the surface. Under appropriate conditions, the setup is found to feature a barrier near the surface which can be employed to levitate particles or used as a trapping or cooling mechanism. Finally, the problem of spontaneous decay [J. Kästel and M. Fleischhauer, Phys. Rev. A **68**, 011804(R) (2005)] is revisited. Disregarding of absorption is shown to drastically falsify the dependence on the atomic position of the decay rate.

PACS numbers: 12.20.-m, 42.50.Wk, 34.35.+a, 42.50.Nn

I. INTRODUCTION

The first most comprehensive account of the properties of left-handed materials (LHMs), i.e., materials simultaneously exhibiting negative real parts of the electric permittivity and the magnetic permeability in a certain frequency interval, was given by Veselago [1]. As he pointed out, a negative refractive index may be attributed to such materials, leading to a number of unusual optical phenomena. While natural materials with a negative real part of the permittivity such as plasmas [2] or a negative real part of the permeability such as some ferrites [3] exist, LHMs have not yet been found in nature. During the last decade, significant progress in the fabrication of LHMs in laboratories has been achieved. Metamaterials based on periodic arrays of split ring resonators and a grid of metallic rods have been reported to exhibit left-handedness in the microwave region [4, 5]. More recently, a two-dimensional material consisting of a metal–insulator–metal waveguide has been experimentally demonstrated to show a negative refractive index in the optical region [6]. The effective permittivity and permeability of such metamaterials, valid on length scales which are sufficiently large in comparison to the elementary building blocks of the material, are determined either theoretically [7, 8] or by means of reflection experiments [9].

As already indicated in Ref. [1], a planar LHM slab with a negative refractive index has the interesting property of being able to focus light—an effect which suggests the possibility of realizing a so-called superlens for subwavelength imaging with a resolution well beyond the diffraction limit [7]. The superlens concept has been a subject of intense discussion [10, 11], and limiting factors such as the finite dimension of the lens [12] or the influence of absorption have been studied [13].

In view of the unusual properties of LHMs, it has also been of interest to study the modifications of dispersion forces in the presence of magneto-electric materials. In particular, the question of whether a left-handedness may lead to a repulsive Casimir force between two magneto-electric plates has been addressed [14]. From the study of van der Waals (vdW) forces on single [15] and between two ground-state atoms [16] in the presence of a planar system exhibiting magneto-electric properties, it has been shown that the attractive/repulsive behavior of the potential is influenced by the strength of the magnetic properties rather than by the left-handedness. This may be attributed to the fact that in both cases the atoms are in the ground state, so the vdW forces represent off-resonant interactions that involve integrals over the whole frequency range. Hence, frequency intervals where no left-handedness occurs will inevitably also contribute to the force and counteract the effect of the left-handedness; this becomes evident after expressing the force in terms of an integral over the imaginary frequency axis where both the permittivity and the permeability are always real and positive. Similar arguments also apply to the abovementioned Casimir force between two magneto-electric plates, where a repulsive behavior has also been found to primarily require strong magnetic rather than left-handed properties [14].

Two strategies might be envisaged to enhance the influence of left-handed properties on dispersion forces.

The first one would be to consider a material exhibiting left-handedness over a sufficiently large (real) frequency range, as recently discussed in the context of the Casimir force [17]; however, such an requirement is, in general, in conflict with the causality requirements met by all physical media. Secondly, one may consider excited systems like amplifying media as also addressed in Ref. [17]. The fundamental difference between absorbing and amplifying media requires, however, a careful reconsideration of the underlying quantum electrodynamics [18]. The situation is more transparent in the case of an excited atom where the necessary theory of vdW forces is readily available [19]. Excited atoms give rise to resonant force components which directly depend on the frequencies of possible downward transitions. If a material exhibits left-handed properties at one such frequency, one may expect these to influence the dispersion forces in a more significant way.

The spontaneous emission of an excited atom situated in vacuum in the vicinity of a perfect mirror combined with a lossless LHM slab is studied in Refs. [20, 21], where it is noticed that a slab of unity negative refraction ($n=-1$) has the peculiar feature of making the space between atom and mirror appear of zero optical length when the atom–slab distance is equal to the thickness of the slab. For such positions, called focal points, complete suppression of the spontaneous emission for a dipole moment parallel to the surface, and enhancement of the spontaneous emission rate by a factor of two for a dipole moment perpendicular to the surface is reported. More recently, it has been pointed out that in reality inhibition of spontaneous decay can be weakened due to nonradiative decay at short distances and due to radiative decay at large distances [22].

Motivated by Refs. [20, 21], we shall study the vdW interaction of an excited two-level atom with the quantized electromagnetic field in the presence of a perfect mirror combined with a realistic LHM slab. To conform with causality and to avoid unphysical consequences, absorption in the LHM is taken into account from the very beginning. The paper is organized as follows. In Sec. II, basic formulas for the vdW potential and the decay rate, and for the Green tensor of a planar magneto-electric multilayer structure are given. Section III is devoted to analytical and numerical studies of the vdW potential experienced by an excited two-level atom in front of a system consisting of a LHM slab combined with a perfect mirror. Special emphasis is put on the effects of material absorption. In Sec. IV, the atomic spontaneous decay rate is discussed and a comparison with earlier results is made. Some concluding remarks and a summary are given in Sec. V.

II. BASIC EQUATIONS

Consider the vdW potential of a neutral, unpolarized and nonmagnetic atomic system [position $\mathbf{r}_A$, energy eigenstate $|n\rangle$, transition frequencies ω_{nk}, electric-dipole transition matrix elements $\mathbf{d}_{nk}$, polarizability $\boldsymbol{\alpha}(\omega)$] in the presence of an arbitrary magneto-electric medium of complex permittivity $\varepsilon(\mathbf{r},\omega)$ and permeability $\mu(\mathbf{r},\omega)$. The medium affects the classical Green tensor $\mathsf{G}(\mathbf{r},\mathbf{r}',\omega)$ of the electromagnetic field, which satisfies the differential equation

$$\left[\boldsymbol{\nabla}\times\frac{1}{\mu(\mathbf{r},\omega)}\boldsymbol{\nabla}\times\ -\frac{\omega^2}{c^2}\varepsilon(\mathbf{r},\omega)\right]\mathsf{G}(\mathbf{r},\mathbf{r}',\omega)=\boldsymbol{\delta}(\mathbf{r}-\mathbf{r}') \tag{1}$$

together with the boundary condition at infinity

$$\mathsf{G}(\mathbf{r},\mathbf{r}',\omega)\to 0 \quad \text{for} \quad |\mathbf{r}-\mathbf{r}'|\to\infty. \tag{2}$$

The potential can be decomposed into a resonant and an off-resonant part (see, e.g., Ref. [19]),

$$U_n(\mathbf{r}_A)=U_n^{\rm r}(\mathbf{r}_A)+U_n^{\rm or}(\mathbf{r}_A), \tag{3}$$

where

$$U_n^{\rm r}(\mathbf{r}_A)= -\mu_0\sum_k\Theta(\omega_{nk})\omega_{nk}^2\mathbf{d}_{nk}\cdot{\rm Re}\,\mathsf{G}^{(1)}(\mathbf{r}_A,\mathbf{r}_A,\omega_{nk})\cdot\mathbf{d}_{kn} \tag{4}$$

(Θ: unit step function) and

$$U_n^{\rm or}(\mathbf{r}_A)=\frac{\hbar\mu_0}{2\pi}\int_0^\infty {\rm d}u\,u^2\,{\rm Tr}\Big[\boldsymbol{\alpha}(iu)\cdot\mathsf{G}^{(1)}(\mathbf{r}_A,\mathbf{r}_A,iu)\Big], \tag{5}$$

respectively. Here, $\mathsf{G}^{(1)}(\mathbf{r},\mathbf{r}',\omega)$ refers to the scattering part of the Green tensor. For an excited atom, the resonant part of the potential often dominates and the off-resonant part can be neglected, as we will do throughout this paper. We shall also be interested in the rate of the spontaneous decay $|n\rangle\to|k\rangle$ of the atom, which reads as (see, e.g., Ref. [23])

$$\Gamma=\Theta(\omega_{nk})\frac{2\omega_{nk}^2}{\hbar\varepsilon_0 c^2}\,\mathbf{d}_{nk}\cdot{\rm Im}\,\mathsf{G}(\mathbf{r}_A,\mathbf{r}_A,\omega_{nk})\cdot\mathbf{d}_{nk}. \tag{6}$$

In what follows, we restrict ourselves to a two-level atom with upper level $|1\rangle$ and lower level $|0\rangle$. Consider the atom to be placed in free space in front of a metamaterial slab of thickness d, permittivity $\varepsilon(\omega)$ and permeability $\mu(\omega)$ which is bounded by a perfectly conducting mirror on the back, as sketched in Fig. 1. The coordinate system is chosen such that the z-axis is perpendicular to the slab and its origin coincides with the slab–vacuum interface. The scattering part of the Green tensor at the relevant atomic transition frequency and equal positions $\mathbf{r}=\mathbf{r}'=\mathbf{r}_A$ in the vacuum region is given by [15]

$$\mathsf{G}^{(1)}(\mathbf{r}_A,\mathbf{r}_A,\omega_{nk})\equiv\mathsf{G}^{(1)}(z_A,z_A,\omega_{10}) =\frac{i}{8\pi^2}\int{\rm d}^2q\,\frac{1}{\beta}\sum_{\sigma=s,p}\mathbf{e}_\sigma^+\mathbf{e}_\sigma^-r_{2-}^\sigma e^{2i\beta z_A}. \tag{7}$$

In Eq. (7), p (s) denotes p- (s-)polarization. The reflection coefficients are given by

$$r^s_{2-} = \frac{r^s_{21} - e^{2i\beta_1 d}}{1 - r^s_{21} e^{2i\beta_1 d}}\,, \tag{8}$$

$$r^p_{2-} = \frac{r^p_{21} + e^{2i\beta_1 d}}{1 + r^p_{21} e^{2i\beta_1 d}}\,, \tag{9}$$

with

$$r^s_{21} = \frac{\mu\beta - \beta_1}{\mu\beta + \beta_1}\,, \quad r^p_{21} = \frac{\varepsilon\beta - \beta_1}{\varepsilon\beta + \beta_1}\,, \tag{10}$$

where the wave vectors in the z direction are given by

$$\beta = \sqrt{\frac{\omega_{10}^2}{c^2} - q^2}\,, \quad \beta_1 = \sqrt{k_1^2 - q^2}\,, \tag{11}$$

with k_1, which always appears in the form of k_1^2 in the Green tensor, Eq. (7), being given according to

$$k_1^2 = \frac{\omega_{10}^2}{c^2}\varepsilon(\omega_{10})\mu(\omega_{10}). \tag{12}$$

The s- and p-polarization unit vectors are defined as

$$\mathbf{e}_s^{\pm} = \mathbf{e}_q \times \mathbf{e}_z, \quad \mathbf{e}_p^{\pm} = \frac{c}{\omega_{10}}(q\mathbf{e}_z \mp \beta\mathbf{e}_q) \tag{13}$$

($\mathbf{e}_q = \mathbf{q}/q$, $q = |\mathbf{q}|$). The square root in Eq. (11) has to be chosen such that it obeys the physical requirement $\operatorname{Im}\beta_1 > 0$ for a passive medium, with this choice being unique for purely absorbing media ($\operatorname{Im}\varepsilon, \operatorname{Im}\mu > 0$) [8]. The imaginary part of β_1^2 reads $\operatorname{Im}\beta_1^2 = (\operatorname{Re}\varepsilon \operatorname{Im}\mu + \operatorname{Im}\varepsilon \operatorname{Re}\mu)\omega_{10}^2/c^2$. It is positive for right-handed materials, which together with the condition $\operatorname{Im}\beta_1 > 0$ implies that β_1 has to be in the first quadrant of the complex plane. On the other hand, $\operatorname{Im}\beta_1^2$ is negative for left-handed materials. This, combined with the condition $\operatorname{Im}\beta_1 > 0$, leads to that β_1 lies in the second quadrant of the complex plane (see also Ref. [24]).

Introduction of polar coordinates in the q-plane, i. e., $\mathbf{e}_q = (\cos\phi, \sin\phi, 0)$, $\mathbf{e}_s^{\pm} = (\sin\phi, -\cos\phi, 0)$, $\mathbf{e}_z = (0, 0, 1)$, implies the identities

$$\mathbf{e}_s^+\mathbf{e}_s^- = \begin{pmatrix} \sin^2\phi & -\sin\phi\cos\phi & 0 \\ -\sin\phi\cos\phi & \cos^2\phi & 0 \\ 0 & 0 & 0 \end{pmatrix} \tag{14}$$

and, with $\mathbf{e}_p^{\pm} = (\mp\beta c\cos\phi/\omega_{10}, \mp\beta c\sin\phi/\omega_{10}, qc/\omega_{10})$,

$$\mathbf{e}_p^+\mathbf{e}_p^- = \frac{c^2}{\omega_{10}^2}\begin{pmatrix} -\beta^2\cos^2\phi & -\beta^2\sin\phi\cos\phi & -q\beta\cos\phi \\ -\beta^2\sin\phi\cos\phi & -\beta^2\sin^2\phi & -q\beta\cos\phi \\ q\beta\cos\phi & q\beta\sin\phi & q^2 \end{pmatrix}. \tag{15}$$

With $\mathrm{d}^2q = q\,\mathrm{d}q\,\mathrm{d}\phi$, the angular integration in Eq. (7) can be performed on using

$$\int_0^{2\pi} \mathrm{d}\phi\, \mathbf{e}_s^+\mathbf{e}_s^- = \pi \begin{pmatrix} 1 & 0 & 0 \\ 0 & 1 & 0 \\ 0 & 0 & 0 \end{pmatrix}, \tag{16}$$

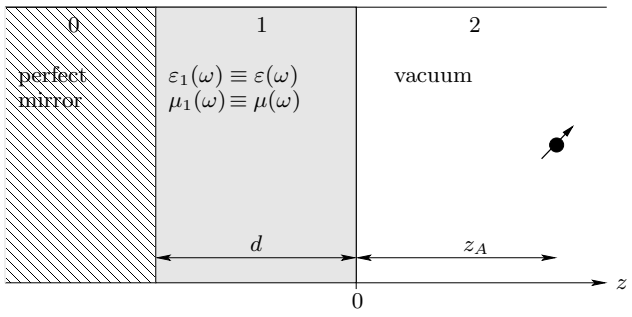

FIG. 1: Atom in a front of a slab of an (absorptive) metamaterial of thickness d which is bounded by a perfect mirror on the back.

FIG. 1: Atom in a front of a slab of an (absorptive) metamaterial of thickness d which is bounded by a perfect mirror on the back.

$$\int_0^{2\pi} \mathrm{d}\phi\, \mathbf{e}_p^+\mathbf{e}_p^- = \frac{\pi c^2}{\omega_{10}^2}\begin{pmatrix} -\beta^2 & 0 & 0 \\ 0 & -\beta^2 & 0 \\ 0 & 0 & 2q^2 \end{pmatrix}, \tag{17}$$

resulting in

$$\mathbf{G}^{(1)}(z_A, z_A, \omega_{10}) = \frac{i}{8\pi}\int_0^{\infty} \mathrm{d}q\, \frac{q}{\beta}\, e^{2i\beta z_A} \times \begin{pmatrix} r^s_{2-} - \frac{\beta^2 c^2}{\omega_{10}^2} r^p_{2-} & 0 & 0 \\ 0 & r^s_{2-} - \frac{\beta^2 c^2}{\omega_{10}^2} r^p_{2-} & 0 \\ 0 & 0 & \frac{2q^2 c^2}{\omega_{10}^2} r^p_{2-} \end{pmatrix}. \tag{18}$$

From Eq. (18) it can be seen that an atom with a dipole moment perpendicular to the surface is coupled to the p-polarized waves only while an atom with a dipole moment parallel to the surface is coupled to both p- and s-polarized waves. It is instructive to decompose the integral in Eq. (18) into two parts,

$$\int_0^{\infty} \mathrm{d}q\, \frac{q}{\beta}\, e^{2i\beta z_A} f(q) = \int_0^{\frac{\omega_{10}}{c}} \mathrm{d}\beta\, e^{2i\beta z_A} f\left(\sqrt{\frac{\omega_{10}^2}{c^2} - \beta^2}\right) + \frac{1}{i}\int_0^{\infty} \mathrm{d}b e^{-2bz_A} f\left(\sqrt{\frac{\omega_{10}^2}{c^2} + b^2}\right). \tag{19}$$

The first integral, which contains an oscillating factor, results from propagating waves, whereas the second one, which contains an exponentially decaying factor, results from evanescent waves. The first is the more important one away from the surfaces while the second dominates near the surfaces.

III. VDW POTENTIAL

A. Ideal (nonabsorbing) LHM

Let us assume hypothetically an absolutely nonabsorbing LHM having $\varepsilon=\mu=-1$. In accordance with the remarks below Eq. (13), we thus set

$$\beta_1 = \begin{cases} -\beta & \text{for } q \le \omega/c, \\ \beta & \text{for } q \ge \omega/c, \end{cases} \tag{20}$$

and the reflection coefficients (8)–(10) become

$$r^s_{2-} = -e^{-2i\beta d}, \quad r^p_{2-} = e^{-2i\beta d}. \tag{21}$$

Note that this result does not depend to the sign of the square root chosen for β_1, since for the ideal LHM discussed here, the reflection coefficients are invariant under a change $\beta_1 \to -\beta_1$. Substitution of these reflection coefficients in Eq. (18) for the Green tensor leads to

$$\begin{aligned} \mathsf{G}^{(1)}(z_A, z_A, \omega_{10}) &= -\frac{i}{8\pi}\int_0^{\omega_{10}/c} \mathrm{d}\beta\, e^{2i\beta(z_A-d)} \\ &\times \begin{pmatrix} 1+\beta^2c^2/\omega_{10}^2 & 0 & 0 \\ 0 & 1+\beta^2c^2/\omega_{10}^2 & 0 \\ 0 & 0 & -2(1-c^2\beta^2/\omega_{10}^2) \end{pmatrix} \\ &- \frac{1}{8\pi}\int_0^{\infty} \mathrm{d}b\, e^{-2b(z_A-d)} \\ &\times \begin{pmatrix} 1-b^2c^2/\omega_{10}^2 & 0 & 0 \\ 0 & 1-b^2c^2/\omega_{10}^2 & 0 \\ 0 & 0 & -2(1+c^2b^2/\omega_{10}^2) \end{pmatrix}. \end{aligned} \tag{22}$$

Equation (22) reveals that for $z_A > d$, the Green tensor exactly coincides with that of a configuration in which a perfectly conducting mirror is placed at $z = d$. As can be seen from an image dipole construction, this is due to the perfect negative refraction taking place at the vacuum–LHM interface: The image of an electric dipole at $z_A > d$ is situated at $z_A^\star = d - (z_A - d)$, just as it would be if a perfectly conducting mirror were placed at $z = d$ (see Fig. 2). An important difference to the case of a mirror placed at $z = d$ is the fact that in the setup considered here the atom can be placed in the region $0 < z_A \le d$. However, it can be seen that, whereas the first integral in Eq. (22), which is complex, is always well-behaved, the second (purely real) integral tends to minus infinity in this region. Thus we are left with an infinite potential for $0 < z_A \le d$, despite the absence of any physical surface at d. We clearly have a situation where an unphysical assumption (of absolute zero absorption) gives rise to unphysical results.

After calculating the two integrals, we obtain for $z_A > d$

$$\begin{aligned} G^{(1)}_{xx}(z_A, z_A, \omega_{10}) &= G^{(1)}_{yy}(z_A, z_A, \omega_{10}) \\ &= \frac{\omega_{10}e^{i\tilde{z}}}{4\pi c\tilde{z}^3}\left(1 - i\tilde{z} - \tilde{z}^2\right), \end{aligned} \tag{23}$$

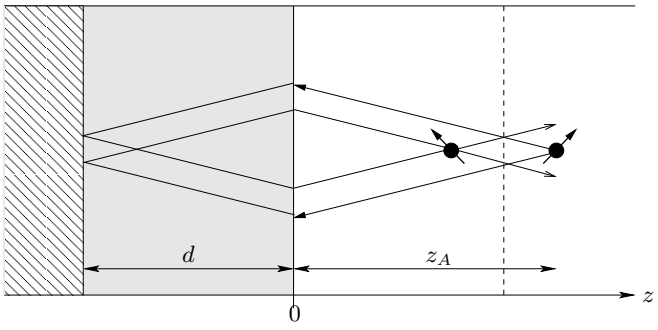

FIG. 2: Image-dipole construction for the setup depicted in Fig. 1. The dashed line marks the position of a perfect mirror that would generate the same image.

$$G^{(1)}_{zz}(z_A, z_A, \omega_{10}) = \frac{\omega_{10}e^{i\tilde{z}}}{2\pi c\tilde{z}^3}\left(1 - i\tilde{z}\right) \tag{24}$$

[$\tilde{z} = 2\omega_{10}(z_A - d)/c$]. Note that the off-diagonal components of the Green tensor are equal to zero. For $z_A > d$, the vdW potential then reads, in accordance with Eqs. (3)–(5) and after neglecting the off-resonant part,

$$\begin{aligned} U(z_A) &\simeq U_1^r(z_A) \\ &= -\mu_0\omega_{10}^2\left[\mathrm{Re}\, G^{(1)}_{xx}|\mathbf{d}^{\parallel}_{10}|^2 + \mathrm{Re}\, G^{(1)}_{zz}|\mathbf{d}^{\perp}_{10}|^2\right] \end{aligned} \tag{25}$$

[$\mathbf{d}^{\parallel}_{10} = ((d_{10})_x, (d_{10})_y, 0)$, $\mathbf{d}^{\perp}_{10} = (0, 0, (d_{10})_z)$], where

$$\mathrm{Re}\, G^{(1)}_{xx} = \frac{\omega_{10}}{4\pi c\tilde{z}^3}\left[\cos(\tilde{z}) + \tilde{z}\sin(\tilde{z}) - \tilde{z}^2\cos(\tilde{z})\right] \tag{26}$$

and

$$\mathrm{Re}\, G^{(1)}_{zz} = \frac{\omega_{10}}{2\pi c\tilde{z}^3}\left[\cos(\tilde{z}) + \tilde{z}\sin(\tilde{z})\right]. \tag{27}$$

For $0 < z_A \le d$, the potential is, as already mentioned, divergent due to the unphysical assumption of vanishing absorption. Hence the question may arise whether at least in the range $z_A > d$ the above-given result can be regarded as being correct in the limit of sufficiently small absorption. An answer to this question can obviously only be given by taking material absorption into account from the very beginning, as shall be done in the next section.

B. Real (absorbing) LHM

To allow for material absorption, we return to Eq. (18) for the scattering part of the Green tensor and set therein $\varepsilon(\omega_{10}) = -1 + i\eta_e$, $\mu(\omega_{10}) = -1 + i\eta_m$, where for simplicity we assume $\eta \equiv \eta_e = \eta_m$. Due to the positive imaginary parts of ε and μ, divergent integrals of the type of the second integral in Eq. (22) can never occur. Note that nonvanishing absorption helps to regularize the behavior of the integrals, just like it does in the superlens geometry [7].

In Fig. 3, the resulting (resonant) vdW potential is plotted versus the distance from the atom to the LHM slab, for the two cases of parallel and perpendicular alignment of the atomic dipole moment with respect to the slab and for different values of absorption. It is seen that the potential features an attractive behavior in the nonretarded regime, which is governed by an inverse power law, while in the retarded regime an oscillating behavior with alternating sign of the potential occurs. The nonretarded regime is dominantly determined by evanescent waves [first integral in Eq. (19)] while propagating waves are mainly responsible for the retarded regime [second integral in Eq. (19)]. The figure further reveals that in the limit of vanishing absorption when η tends to zero, then the potential approaches the one found, for $z_A > d$, in the case of absolutely nonabsorbing LHM [Eq. (25) together with Eqs. (26) and (27)]. It is clearly seen that in practice unavoidable absorption always prevents the system to feature an infinitely negative potential in the interval $0 < z_A \leq d$, as would be expected from the study of a nonabsorbing LHM. We do, however, note that for very small absorption, the potential starts to become strongly negative around the region $z_A \approx d$, where this effect is more noticeable on the case of perpendicular atomic dipole moment.

A very striking feature of the potential is completely missing if absorption is disregarded: For a transition dipole moment parallel to the surface and medium absorption, a barrier appears in front of the slab at distances $z_A\omega_{10}/c \lesssim 1$ [Fig. 3(a), $10^{-4} \lesssim \eta \lesssim 10^{-3}$]. The fact that barriers occur only for transition dipole moments parallel to the surface but not for those perpendicular to the surface suggests that s-polarized waves, which are coupled to the first but not the latter, play an important role in their formation.

For sufficiently weak absorption [$\eta = 10^{-5}$ in Fig. 3(a) and $\eta = 10^{-3}, 10^{-4}, 10^{-5}$ in Fig. 3(b)], an attractive potential starts to appear at distances of a few wavelengths, somewhat away from the surface. Atoms located within this range will get adsorbed to the surface. This behavior is more pronounced for a transition dipole moment perpendicular to the surface than for a transition dipole moment parallel to the surface—a fact that can be related to the coupling respective no coupling of these two dipole moment orientations to s-polarized waves. By setting the denominators in Eqs. (8) and (9) equal to zero, one finds that the poles of the generalized reflection coefficients for p- and s-polarized waves, respectively, are solutions to the equations

$$\frac{\beta_1}{\varepsilon\beta} = \coth(i\beta_1 d), \tag{28}$$

$$\frac{\beta_1}{\mu\beta} = \tanh(i\beta_1 d). \tag{29}$$

These are the dispersion relations for the surface plasmon polaritons [25], which can be strongly excited when the atom is close to the surface. The real parts of the poles lie in the regions covered by the second integral in

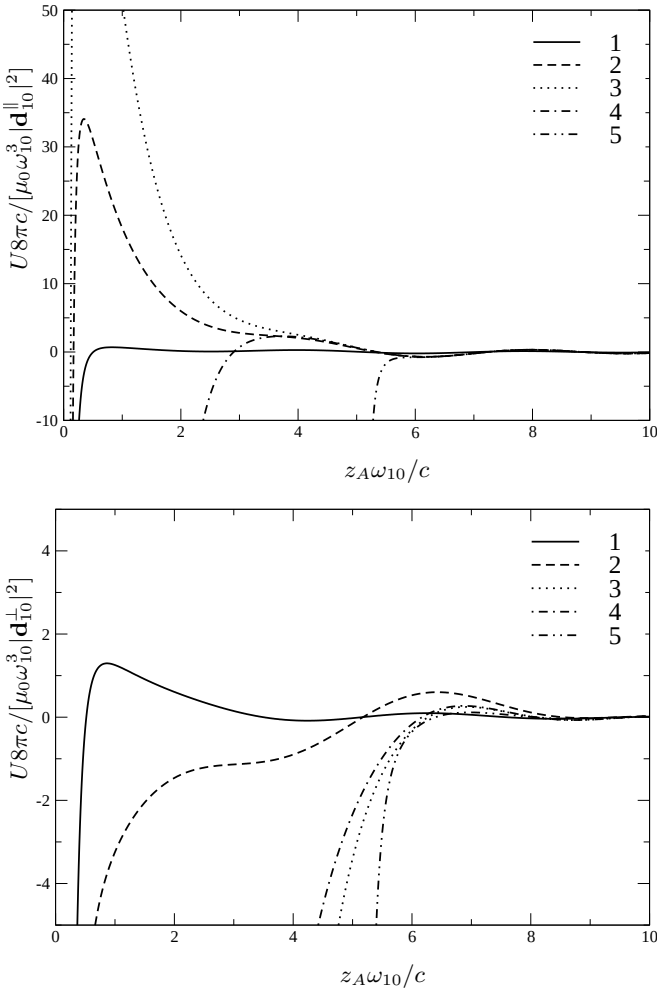

FIG. 3: Resonant VdW potential experienced by an excited two-level atom in the setup sketched in Fig. 1 for $d = 5c/\omega_{10}$, $\varepsilon(\omega_{10}) = \mu(\omega_{10}) = -1 + i\eta$, and (a) dipole moments parallel to the surface and (b) dipole moments perpendicular to the surface. Curves 1–5 refer to various degrees of absorption $\eta = 10^{-1}$, 10^{-3}, 10^{-4}, 10^{-5} and 0, respectively.

Eq. (19). The poles of the s- (p-)polarized waves are in the upper (lower) half of the complex plane, where for smaller absorption they are closer to the real axis.

The influence on the vdW potential of the slab thickness is illustrated in Fig. 4. Note that zero slab thickness means an atom in front of a perfect mirror. As the slab thickness increases, a potential barrier arises and grows in height for dipole moments parallel to the surface. However, at some threshold value of d, the height of the barrier starts to be reduced, and eventually the barrier disappears when the slab is too thick. This can be explained as resulting from the increasing effects of material absorption. It is seen from the figures that the distance from the surface at which a relatively strong attractive potential can occur increases with the slab thickness. This is more pronounced for perpendicular dipole moments rather than for parallel ones—a consequence of

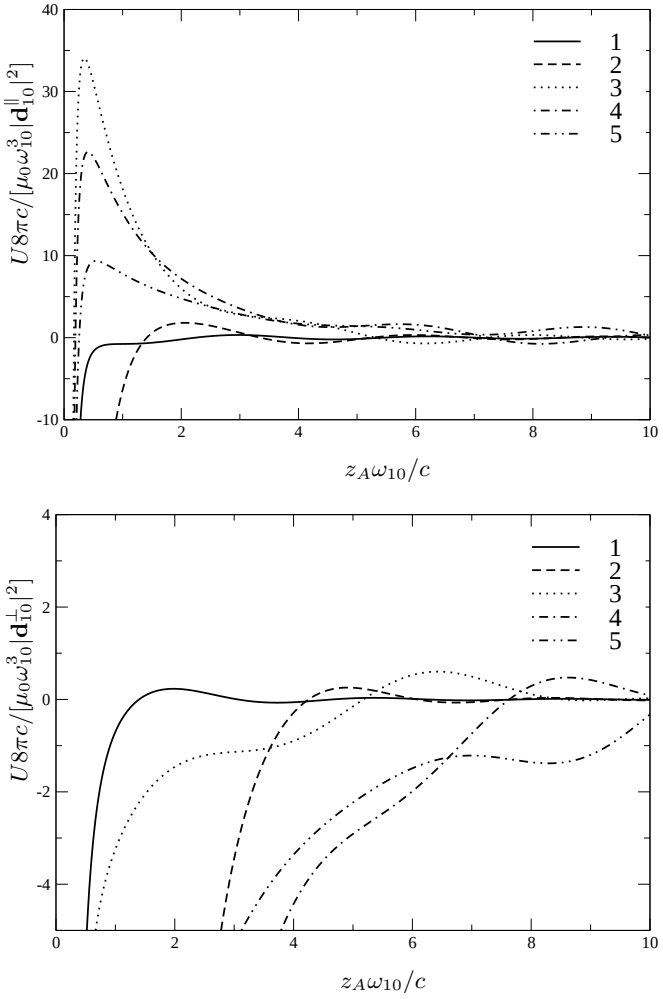

FIG. 4: Resonant vdW potential experienced by an excited atom in the setup sketched in Fig. 1 for $\varepsilon(\omega_{10}) = \mu(\omega_{10}) = -1 + i10^{-3}$, and (a) dipole moments parallel to the surface and (b) dipole moments perpendicular to the surface. Curves 1–5 refer to various thicknesses of the slab $d\omega_{10}/c = 0$, 3, 5, 7 and 10, respectively.

the fact that, as already mentioned, the first is coupled more efficiently to the evanescent waves.

C. Near-surface limit

Further insight into how the appearance of the barrier depends on the amount of absorption, the orientation of the atomic dipole moment as well as the thickness of the LHM slab can be gained by examining the vdW potential in the near-surface limit. Near the surface, the evanescent waves dominate the potential [the second integral in Eq. (19)]. Let us consider the (resonant part of the) potential as given by Eq. (4) together with Eqs. (18) and (19) for very short distances, $z_A\omega_{10}/c \ll 1$, in more detail. The main contribution to the q-integral is from values $q \gg \omega_{10}/c$ and $q \gg \sqrt{|\varepsilon\mu|}\omega_{10}/c$ [$\varepsilon \equiv \varepsilon(\omega_{10})$, $\mu \equiv \mu(\omega_{10})$], since the exponential factor [in the second integral in Eq. (19)] effectively limits the integration interval to values $q \lesssim z_A$. Hence, with

$$\beta \simeq iq, \quad \beta_1 \simeq iq \tag{30}$$

the potential in the short-distance regime reads

$$U(z_A) = -\frac{\omega_{10}^2\mu_0}{8\pi}\int_0^\infty \mathrm{d}q\, e^{-2qz_A} \times\left[\left(\mathrm{Re}\, r_{2-}^s + \frac{q^2c^2}{\omega_{10}^2}\,\mathrm{Re}\, r_{2-}^p\right)|\mathbf{d}_{10}^{\parallel}|^2 + \frac{2q^2c^2}{\omega_{10}^2}\,\mathrm{Re}\, r_{2-}^p|\mathbf{d}_{10}^{\perp}|^2\right], \tag{31}$$

where

$$\mathrm{Re}\, r_{2-}^p = \left[\left(|\varepsilon|^2-1\right)\left(1+e^{-4qd}\right) + \left(|\varepsilon-1|^2+|\varepsilon+1|^2\right)e^{-2qd}\right]\left|\varepsilon+1+(\varepsilon-1)e^{-2qd}\right|^{-2}, \tag{32}$$

$$\mathrm{Re}\, r_{2-}^s = \left[\left(|\mu|^2-1\right)\left(1+e^{-4qd}\right) - \left(|\mu-1|^2+|\mu+1|^2\right)e^{-2qd}\right]\left|\mu+1-(\mu-1)e^{-2qd}\right|^{-2}. \tag{33}$$

When

$$\varepsilon \simeq -1 \quad \text{and} \quad \mu \simeq -1, \tag{34}$$

then the first terms in Eqs. (32) and (33) approximately vanish, thus

$$\mathrm{Re}\, r_{2-}^p \simeq \frac{\left(|\varepsilon-1|^2+|\varepsilon+1|^2\right)e^{-2qd}}{\left|\varepsilon+1+(\varepsilon-1)e^{-2qd}\right|^2}, \tag{35}$$

$$\mathrm{Re}\, r_{2-}^s \simeq -\frac{\left(|\mu-1|^2+|\mu+1|^2\right)e^{-2qd}}{\left|\mu+1-(\mu-1)e^{-2qd}\right|^2}, \tag{36}$$

where the opposite signs imply that the two polarizations give competing contributions to the potential. Namely, the p-polarized waves give rise to attractive contributions to the potential while the s-polarized waves lead to repulsive ones. Very close to the surface, due to the presence of the q^2 factor [see Eq. (31)], the contribution to the potential of the p-polarized waves is proportional to $1/z_A^3$ while the contribution of the s-polarized waves is proportional to $1/z_A$. The contribution of the p-polarized waves hence dominates, resulting in an attractive potential (also see Figs. 3 and 4). At some distance from the surface, the contribution of the s-polarized waves can dominate under appropriate conditions, which then leads to the appearance of a potential barrier. This also explains the absence of the barrier in the case where the dipole moment is perpendicular to the surface.

Inspection of Eqs. (32) and (33) reveals that $\mathrm{Re}\, r_{2-}^p$ is positive for all $|\varepsilon| \geq 1$ while $\mathrm{Re}\, r_{2-}^s$ is negative for all

$|\mu| \geq 1$. Since the height of the potential barrier is determined by the magnitude of $|\mathrm{Re}\, r^s_{2-}|$, lefthandedness is not necessarily required to realize a potential barrier in general. We note here yet another situation where, in the absence of the lefthandedness property, a high potential barrier might appear. For this it is convenient to consider a more general setup where the spatial area 2 in Fig. 1 is filled with a medium of permittivity $\varepsilon_2(\omega)$ and permeability $\mu_2(\omega)$. Then, apart from a scaling factor due to local-field correction, $9\varepsilon_2^2(\omega_{10})/[2\varepsilon_2(\omega_{10})+1]^2$ [26], the vdW potential retains the form of Eq. (31), with the reflection coefficients (32) and (33) being modified as follows: $|\varepsilon|^2-1$ ($|\mu|^2-1$) is replaced by $|\varepsilon|^2-|\varepsilon_2|^2$ ($|\mu|^2-|\mu_2|^2$) and $\varepsilon \pm 1$ ($\mu \pm 1$) is replaced by $\varepsilon \pm \varepsilon_2$ ($\mu \pm \mu_2$). If we choose $|\varepsilon| > |\varepsilon_2|$ and $|\mu| < |\mu_2|$, the first terms, rather than the second terms, in the modified equations (32) and (33) dominate, but it remains that p- (s-)polarized waves give rise to an attractive (repulsive) potential. In this scenario, the appearance and the height of the barrier are determined by the difference between the absolute values of the permittivity on the two sides of the interface and the accordant difference between the absolute values of the permeability. Negative (real parts of the) permittivities and/or permeabilities are allowed but not a prerequisite. The presence of a potential barrier in this case is essentially a surface effect, the finite thickness of the slab and the perfect mirror playing only secondary roles.

Let us return to the influence of the thickness of the LHM slab. As can be inferred from Eq. (33), the magnitude of $|\mathrm{Re}\, r^s_{2-}|$ is about 1 for $d \to 0$ (slab absent), and is typically determined by a e^{2qd} term otherwise. Therefore the presence of the slab is crucial for the appearance of a potential barrier. When the slab is very thick, the influence of the mirror vanishes $e^{-2qd} \to 0$ [cf. Eqs. (32) and (33)], and it is not difficult to verify that Eq. (31) reproduces the result for the resonant part of the potential of an excited atom in front of an interface (see, e.g., Ref. [19]), which, in the nonretarded limit reads as

$$U(z_A) = -\frac{C}{z_A^3}\frac{|\varepsilon|^2-1}{|\varepsilon+1|^2} \tag{37}$$

[$C = [|\mathbf{d}^{\parallel}_{10}|^2 + 2|\mathbf{d}^{\perp}_{10}|^2]/(32\pi\varepsilon_0)$]. Clearly, when the slab is too thick, then the atom only feels the vacuum–slab interface. Note that a repulsive behavior of the potential is also possible in the case of non-magnetic materials provided that $|\varepsilon| < 1$. It is particularly apparent that $|U(z_A)|$ cannot become infinity as $z_A \to 0$, because the underlying macroscopic quantum electrodynamics is valid only for atom–surface distances much larger than the average distances between the constituents of the media involved.

Although potential barriers in planar magnetodielectric multilayer structures have also been found in the case of ground-state atoms [15], it is worth noting that the barriers are generally much more significant in the case of excited atoms. For instance, the peaks of the potentials in the numerical examples given here are about 6 orders of magnitude larger than those given in Ref. [15]. This is because the potential in the case of ground-state atoms is an integral over the whole frequency range, for most of which the material does not exhibit strong electric or magnetic responses. The excited atoms essentially allows one to pick out a frequency of choice.

IV. SPONTANEOUS DECAY RATE REVISITED

Whereas the (resonant) vdW potential depends on the real part of the Green tensor, the rate of spontaneous decay is determined by its imaginary part. From Eq. (22) for the Green tensor of the absolutely nonabsorbing setup considered in Sec. III A, it can be seen that the contributions from evanescent waves, which give rise to divergences in the region $z_A \leq d$, are purely real and thus do not contribute to the decay rate. The decay rate is thus expressed in terms of traveling-wave contributions which are finite for arbitrary z_A. However, baring in mind the findings for the vdW potential, one should carefully examine whether these idealized results valid for nonabsorbing material are an appropriate approximation to the reality.

To do so, we note that from Eq. (6), the decay rate can be rewritten as

$$\frac{\Gamma}{\Gamma_0} = 1 + \frac{6\pi c}{\omega_{10}|\mathbf{d}_{10}|^2}\,\mathrm{Im}\left[G^{(1)}_{xx}|\mathbf{d}^{\parallel}_{10}|^2 + G^{(1)}_{zz}|\mathbf{d}^{\perp}_{10}|^2\right], \tag{38}$$

where

$$\Gamma_0 = \frac{|\mathbf{d}_{10}|^2\omega_{10}^3}{3\pi\hbar\varepsilon_0 c^3} \tag{39}$$

is the decay rate of the atom in free space. Let us first assume an absolutely nonabsorbing LHM having $\varepsilon = \mu = -1$ again. From Eqs. (23) and (24) we obtain

$$\mathrm{Im}\, G^{(1)}_{xx} = \frac{\omega_{10}}{4\pi c\tilde{z}^3}\left[\sin(\tilde{z}) - \tilde{z}\cos(\tilde{z}) - \tilde{z}^2\sin(\tilde{z})\right], \tag{40}$$

$$\mathrm{Im}\, G^{(1)}_{zz} = \frac{\omega_{10}}{2\pi c\tilde{z}^3}\left[\sin(\tilde{z}) - \tilde{z}\cos(\tilde{z})\right] \tag{41}$$

[$\tilde{z} = 2\omega_{10}(z_A - d)/c$]. Equation (38) together with Eqs. (40) and (41), which mathematically holds for any atom–surface distance, is studied in Ref. [20]. It is not difficult to see that $\mathrm{Im}\, G^{(1)}_{xx}$ and $\mathrm{Im}\, G^{(1)}_{zz}$ are even functions of $\tilde{z}$, and are finite at the surface. The position $z_A = d$, termed focus point in Ref. [20], stands out in that the optical path for a ray of light for a round trip to the mirror and back is zero. For $z_A = d$, Eq. (38) together with Eqs. (40) and (41) implies complete inhibition of spontaneous decay ($\Gamma = 0$) for a dipole moment oriented parallel to the surface and enhancement of spontaneous decay ($\Gamma = 2\Gamma_0$) for dipole moment oriented perpendicular to the surface [20].

It is worth noting that absorption can drastically change this behavior. Inclusion in the calculations of

the effect of material absorption requires the calculations to be performed on the basis of the exact (scattering part of the) Green tensor as given in Eq. (18) together with Eqs. (8)–(10). Numerical examples are given in Fig. 5, where the case of zero absorption in accordance with Eqs. (38)–(41) is also shown to facilitate comparison. We see that, whereas in the case of strictly zero absorption the decay rate as a function of the atomic position $z_A > 0$ is symmetric with respect to the position $z_A = d$, any absorption destroys this symmetry. As a result, large enhancement of the spontaneous decay can be observed when the atom is near the surface, which is obviously due to the absorption-assisted atomic coupling with evanescent waves—an effect already known for ordinary materials (see, e.g., Ref. [27]) which features qualitatively new distance terms [cf. Eq. (45)]. This result is consistent with those reported in Ref. [22]. In particular for distances $z_A \leq d$, Eq. (38) together with Eqs. (40) and (41) can not be regarded as an acceptable approximation to the spontaneous decay rate in the case of small absorption—a result which corresponds, for $z_A < d$, to the result found in the case of the vdW potential.

To further elucidate the influence of the evanescent waves, let us examine the near-surface limit of the rate of spontaneous decay. By using approximations similar to those in Sec. III C, it can be shown that for $z_A\omega_{10}/c \ll 1$

$$\frac{\Gamma}{\Gamma_0} = 1 + \frac{3c}{4\omega_{10}|\mathbf{d}_{10}|^2}\int_0^\infty \mathrm{d}q\, e^{-2qz_A}\Big[\Big(\mathrm{Im}\, r^s_{2-} + \frac{q^2c^2}{\omega_{10}^2}\,\mathrm{Im}\, r^p_{2-}\Big)|\mathbf{d}^{\parallel}_{10}|^2 + \frac{2q^2c^2}{\omega_{10}^2}\,\mathrm{Im}\, r^p_{2-}|\mathbf{d}^{\perp}_{10}|^2\Big], \quad (42)$$

where

$$\mathrm{Im}\, r^s_{2-} = \frac{2\mathrm{Im}\mu(1-e^{-4qd})}{|\mu+1-(\mu-1)e^{-2qd}|^2}, \quad (43)$$

$$\mathrm{Im}\, r^p_{2-} = \frac{2\,\mathrm{Im}\,\varepsilon\,(1-e^{-4qd})}{|\varepsilon+1-(\varepsilon-1)e^{-2qd}|^2}. \quad (44)$$

Note that in this case only evanescent waves contribute to the rate. Unlike the real parts [cf. Eqs. (32) and (33)], the imaginary parts of r^s_{2-} and r^p_{2-} have the same (positive) sign. The two polarizations therefore contribute constructively to the spontaneous decay rate. If the slab becomes sufficiently thick, Eq. (42) reduces, in leading order, to

$$\frac{\Gamma}{\Gamma_0} = 1 + \frac{D}{z_A^3}\frac{\mathrm{Im}\,\varepsilon}{|\varepsilon+1|^2} \quad (45)$$

[$D = 3c^3[|\mathbf{d}^{\parallel}_{10}|^2 + 2|\mathbf{d}^{\perp}_{10}|^2]/(8\omega_{10}^3|\mathbf{d}_{10}|^2)$], i.e., the spontaneous rate for an atom in front of an interface. Equation (45) shows that the decay rate takes on large values as $z_A \to 0$, which is a consequence of direct energy transfer from the atom to the constituents of the medium (see, e.g., Ref. [27]).

It is well known that lefthandedness of the slab is of course not a necessary condition for, say, inhibition of spontaneous decay, as illustrated in Fig. 6. The figure shows that almost complete inhibition of spontaneous decay is possible for both parallel and perpendicular orientations of the dipole moment with respect to the surface of a slab that is not lefthanded.

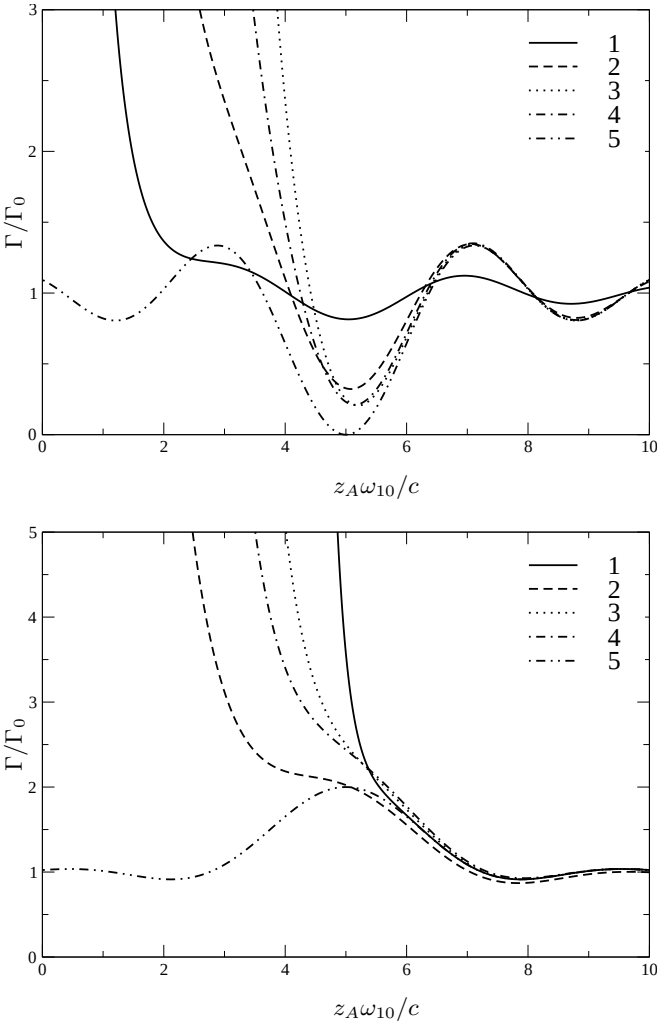

FIG. 5: Atom–surface distance dependence of the decay rate of an excited atom in the setup in Fig. 1 for $\varepsilon = \mu = -1 + i\eta$, $d = 5c/\omega_{10}$, and (a) dipole moments parallel to the surface and (b) dipole moments perpendicular to the surface. Curves 1–5 refer to various degrees of absorption $\eta = 10^{-1}$, 10^{-3}, 10^{-4}, 10^{-5} and 0, respectively.

V. CONCLUDING REMARKS AND SUMMARY

The macroscopic theory employed in this paper breaks down on length scales which are comparable to the size of the elementary building blocks of the metamaterial employed. In order to observe the predicted effects, one thus has to ensure that both the atomic transition wavelength and the atom–surface separation are larger than this

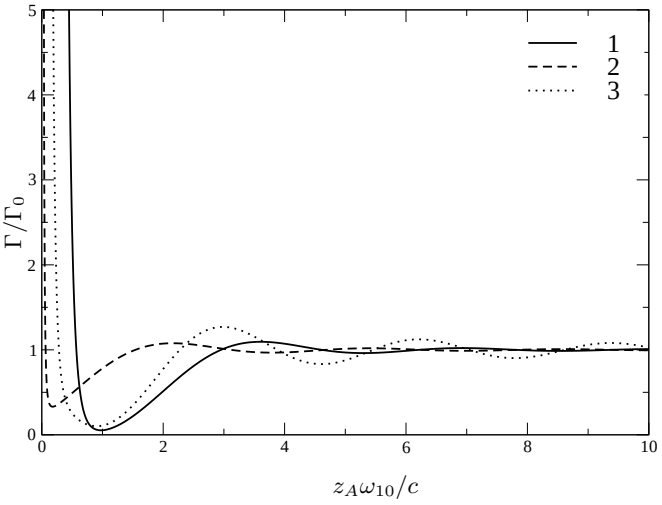

FIG. 6: Atom–surface distance dependence of the decay rate of an excited atom in the setup in Fig. 1 for $d = 5c/\omega_{10}$, and (1) $\varepsilon = 1$, $\mu = -1 + i10^{-3}$, and atomic dipole moment perpendicular to the surface; (2) $\varepsilon = -1 + i10^{-3}$, $\mu = 1$, and atomic dipole moment perpendicular to the surface; (3) $\varepsilon = 1$, $\mu = -1 + i10^{-3}$, and atomic dipole moment parallel to the surface.

length scale. With currently available metamaterials, this can most readily be achieved with polar molecules whose rotational and vibrational transition wavelengths can be very large. For example, the bulk meta-material reported in Ref. [9] exhibits negative refraction with $\mathrm{Re}\, n \approx -1.6$ at a frequency of 1.03 THz; it consists of unit cells with lattice constant $a \approx 6 \times 10^{-5}$m. The frequency of the first rotational transition of a NH molecule (about 1 THz [28]) falls within this frequency window, with the associated wavelength being sufficiently large in comparison with the lattice constant. One could expect the macroscopic results to be valid down to molecule–surface separations of $z_A = 10^{-4}$m, which corresponds to $z_A\omega_{nk}/c \approx 2$. Smaller values of $z_A\omega_{nk}/c$ can be reached by using molecules with larger transition wavelengths.

Let us briefly comment on the strength of the force $F(z_A) = -\partial U(z_A)/\partial z_A$ associated with a potential of the type shown in Figs. 3 and 4. In this context, it may be convenient to express the potential and the force in terms of the spontaneous decay rate Γ. From Eqs. (3), (4), and (39) it follows that $U(z_A) = -3/2\hbar\Gamma_0\lambda_{10}\mathrm{Re}\, G^{(1)}_{xx}(z_A, z_A, \omega_{10})$, where a dipole moment parallel to the surface has been assumed. Consider an excited hydrogen-like atom with a transition having spontaneous decay rate $\Gamma_0 \sim 6 \times 10^8\,\mathrm{s}^{-1}$ and wavelength $\lambda_{10} \sim 10^{-7}\,\mathrm{m}$ [29]. If the atom is at rest relative to the slab, the force that can counter the gravitation force and so levitate the atom has to be larger than $mg = 3 \times 10^{-26}\,\mathrm{N}$. This can be achieved easily. For example, the peak value of the force corresponding to the potential barrier represented by the dotted line in Fig. 3(a) is $10^{-16}\,\mathrm{N}$.

Consider now a situation where one has a sample of a dilute gas of excited atoms at some temperature. Take again hydrogen-like atoms with the same excited level as above. At a temperature of $T = 10\,\mathrm{K}$, the kinetic energy of each particle is $E = 3kT/2 \sim 2 \times 10^{-22}\,\mathrm{J}$. A LHM slab of thickness $d\omega_{10}/c = 9$, permittivity and permeability $\varepsilon = \mu = -1 + i2 \times 10^{-6}$ then provides a potential barrier of a height of $U = 3 \times 10^{-22}\,\mathrm{J}$. This potential barrier is high enough to levitate the sample of the dilute atomic gas. With an appropriate arrangement, it clearly can be employed as a trapping mechanism. One may also think of an (evaporative) cooling apparatus. The kinetic energy is an averaged quantity. Some atoms among the gas sample can have kinetic energy exceeding the average and higher than the potential barrier. These can overcome the barrier and get adsorbed by the walls, in so doing lowering the average kinetic energy of the remaining (a little more diluted) gas sample. It should be pointed out that in the examples meta-materials with very small absorption are assumed, which are still beyond the reach of today's experimental techniques. Furthermore, since excited atoms are considered, the effects predicted hold only for time periods short compared to the atomic lifetime. A more refined theory should include the broadening and shifting of the atomic transition frequency.

In summary, we have studied the resonant vdW potential experienced by an excited two-level atom in front of a meta-material slab backed by a perfect mirror, with emphasis on a LHM slab with unity negative real part of both the permittivity and the permeability, and an atom located in vacuum. We have shown that material absorption has to be taken into account in order to avoid divergent values of the potential when the atom–surface separation becomes smaller than the slab thickness. Only for values of the atom–surface separation which are larger than the slab thickness, disregarding of absorption leads to reasonable results provided that absorption is sufficiently small.

Further, we have shown that the setup can be used to form potential barriers for excited atoms – barriers that are typically of several orders of magnitude higher than those observed for ground-state atoms. In particular, they are significant enough to suggest potential use in quantum levitation, trapping, or cooling of atoms. The barriers are results of competing contributions from s- and p-polarized waves, thus are peculiar to atoms with dipole moments parallel to the surface. For random atomic dipole moment orientations, a corresponding averaging has to be applied which may lead to a reduction of the barrier height.

Finally, we have revisited the effect of the LHM slab on the spontaneous decay of the excited atom. We have shown that already an arbitrarily small but finite amount of material absorption can drastically change the decay compared to that predicted when absorption is ignored. In particular near the surface, absorption gives rise to a noticeable enhancement of the decay. As a prospective task, the theory could be expanded to other systems such as spherically or cylindrically symmetric ones, am-

plifying instead of absorbing media could be assumed, and the vdW interaction between excited atoms near a macroscopic body of meta-material could be investigated.

Acknowledgments

The work was supported by Deutsche Forschungsgemeinschaft. We acknowledge funding from the Alexander von Humboldt Foundation (H.T.D. and S.Y.B.) and the Vietnamese Basic Research Program (H.T.D.).

[1] V. G. Veselago, Sov. Phys. Usp. **10**, 509 (1968).
[2] D. A. Gurnett and A. Bhattacharjee, *Introduction to plasma physics: with space and laboratory application* (Cambridge Univ. Press, 2006).
[3] D. L. Mills and E. Burstein, Rep. Progr. Phys. **37**, 817 (1974).
[4] D. R. Smith, W. J. Padilla, D. C. Vier, S. C. Nemat-Nasser, and S. Schultz, Phys. Rev. Lett. **84**, 4184 (2000).
[5] R. A. Shelby, D. R. Smith, S. C. Nemat-Nasser, and S. Schultz, App. Phys. Lett. **78**, 489 (2001).
[6] H. J. Lezec, J. A. Dionne, and H. A. Atwater, Sci. **316**, 430 (2007).
[7] J. B. Pendry, A. J. Holden, D. J. Robbins, and W. J. Stewart, IEEE Trans. Microwave Theory Tech. **47**, 2075 (1999).
[8] A. P. Vinogradov, A. V. Dorofeenko, and S. Zouhdi, Phys. Usp. **51**, 485 (2008).
[9] O. Paul, C. Imhof, B. Reinhard, R. Zengerle, and R. Beigang, Opt. Expr. **16**, 6736 (2008).
[10] P. G. Kik, S. A. Maier, and H. A. Atwater, Phys. Rev. B. **69**, 045418 (2004).
[11] S. A. Ramakrishna and J. B. Pendry, Phys. Rev. B **67**, 201101 (2003).
[12] J. J. Chen, T. M. Grzegorczyk, B.-I. Wu, and J. A. Kong, Phys. Rev. E **74**, 046615 (2006).
[13] D. R. Smith, D. Schurig, M. Rosenbluth, and S. Schultz, App. Phys. Lett. **82**, 1506 (2003).
[14] C. Henkel and K. Joulain, Europhys. Lett. **72**, 929 (2005).
[15] S. Y. Buhmann, D.-G. Welsch, and T. Kampf, Phys. Rev. A **72**, 032112 (2005).
[16] S. Spagnolo, D. A. R. Dalvit, and P. W. Milonni, Phys. Rev. A **75**, 052117 (2007).
[17] U. Leonhardt and T. G. Philbin, N. J. of Phys. **9**, 254 (2007).
[18] C. Raabe and D.-G. Welsch, The Eur. Phys. J. - Special Topics **160**, 371 (2008).
[19] S. Y. Buhmann, L. Knöll, D.-G. Welsch, and H. T. Dung, Phys. Rev. A **70**, 052117 (2004).
[20] J. Kästel and M. Fleischhauer, Laser Phys. **15**, 135 (2005).
[21] J. Kästel and M. Fleischhauer, Phys. Rev. A **71**, 011804(R) (2005).
[22] J.-P. Xu, Y.-P. Yang, H. Chen, and S.-Y. Zhu, Phys. Rev. A **76**, 063813 (2007).
[23] H. T. Dung, S. Y. Buhmann, L. Knöll, D.-G. Welsch, S. Scheel, and J. Kästel, Phys. Rev. A **68**, 043816 (2003).
[24] S. A. Ramakrishna and O. J. F. Martin, Opt. Lett. **30**, 2626 (2005).
[25] R. Ruppin, J. Phys. Condens. Matter **13**, 1811 (2001).
[26] A. Sambale, S. Y. Buhmann, D.-G. Welsch, and M.-S. Tomaš, Phys. Rev. A **75**, 042109 (2007).
[27] W. Vogel and D.-G. Welsch, *Quantum Optics, 3rd edition* (Wiley-VCH, Weinheim, 2006), auflage: 3rd rev&ex ed.
[28] S. Y. Buhmann, M. Tarbutt, S. Scheel, and E. A. Hinds, *Surface-induced heating of cold polar molecules*, arxiv:0806.2913 [quant-ph] (2008), URL `http://arxiv.org/pdf/0806.2913`.
[29] NIST, *Phys. lab. Physical reference data*, http://physics.nist.gov/PhysRefData/ASD/index.html (last update: June 2004).